STIMULATORY EFFECT OF INSULIN ON GLUCOSE UPTAKE BY MUSCLE INVOLVES THE CENTRAL NERVOUS SYSTEM IN INSULIN-SENSITIVE MICE

4

Claudia P. Coomans
Nienke R. Biermasz
Janine J. Geerling
Bruno Guigas
Patrick C.N. Rensen
Louis M. Havekes
Johannes A. Romijn

Diabetes 2011

ABSTRACT

Insulin inhibits endogenous glucose production (EGP) and stimulates glucose uptake in peripheral tissues. Hypothalamic insulin signaling is required for the inhibitory effects of insulin on endogenous glucose production. We examined the contribution of central insulin signaling on circulating insulin-stimulated tissue-specific glucose uptake. Tolbutamide, an inhibitor of ATP-sensitive potassium channels, or vehicle was infused into the lateral ventricle in the basal state and during hyperinsulinemic-euglycemic conditions in postabsorptive, chow fed C57Bl/6J mice and in postabsorptive, diet-induced obese C57Bl/6J mice. Whole body glucose uptake was measured by D-[^{14}C]glucose kinetics and tissue-specific glucose uptake by 2-deoxy-D-[^{3}H] glucose uptake.

During clamp conditions, intracerebroventricular (i.c.v.) administration of tolbutamide impaired the ability of insulin to inhibit EGP by ~20%. In addition, i.c.v. tolbutamide diminished insulin-stimulated glucose uptake in muscle (by ~59%), but not in heart or adipose tissue. In contrast, in diet-induced obese, insulin resistant mice, i.c.v tolbutamide did not affect the effects of insulin during clamp conditions on EGP or glucose uptake by muscle.

In conclusion, insulin stimulates glucose uptake in muscle in part through effects via ATP-sensitive potassium channels in the central nervous system, in analogy with the inhibitory effects of insulin on EGP. High-fat diet-induced obesity abolished the central effects of insulin on liver and muscle. These observations stress the role of central insulin resistance in the pathophysiology of diet-induced insulin resistance.

INTRODUCTION

In response to nutrients, insulin is rapidly released from pancreatic β-cells and decreases plasma glucose levels by inhibiting endogenous glucose production (EGP) and stimulating glucose transport into skeletal muscle, heart and white adipose tissue (WAT). Intake of high-fat diets can lead to insulin resistance, which plays a primary pathophysiological role in the development of T2DM (1;2). Insulin resistance in the liver results in a decreased capacity of insulin to suppress EGP, whereas insulin resistance in peripheral tissues, including muscle, results in reduced insulin-mediated glucose uptake.

In addition to direct effects of insulin on peripheral tissues, insulin acts in the hypothalamus, where it exerts anorexigenic properties by stimulating proopiomelanocortin (POMC)/cocaine and amphetamine regulated transcript (CART) neurons and by inhibiting agouti-related peptide (AgRP)/neuropeptide Y (NPY) neurons (3-5). In fact, hypothalamic insulin signaling appeared necessary for the inhibitory effect of insulin on EGP (6-8). Insulin activates ATP-sensitive potassium channels (K_{ATP} channels) in neurons of the hypothalamus, including POMC/CART- and AgRP/NPY expressing neurons (9;10). Inhibition of these neuronal K_{ATP} channels by intracerebroventricular (i.c.v.) administration of sulfonylurea (either tolbutamide or glibenclamide) impairs the inhibitory effect of insulin on EGP (7). Conversely, activation of hypothalamic K_{ATP} channels enhances insulin-mediated inhibition of EGP (11).

Although the importance of this central action of insulin for the inhibition of EGP is now well established, the role of the central effects of insulin on glucose disposal is still unknown. Therefore, the aim of the present study was to determine the role of the central effect of insulin on tissue-specific insulin-stimulated glucose disposal in mice without and with diet-induced insulin resistance. To this end, we infused tolbutamide, an inhibitor of K_{ATP} channels, into the lateral ventricle and quantified glucose disposal in mice on a regular diet, both in the basal state and during hyperinsulinemic-euglycemic conditions. We show that the central effects of insulin are not only required for inhibition of EGP, but also enhances insulin-mediated glucose uptake in muscle. Furthermore, we show that these central effects of insulin on EGP and tissue-specific uptake of glucose are lost in diet-induced obese mice, stressing the role of central insulin resistance in the pathophysiology of diet-induced insulin resistance.

MATERIALS AND METHODS

Animals

Male C57Bl/6J mice (15 weeks old) were housed in a temperature-controlled room on a 12-hour light-dark cycle. Animals had free access to water and diet (chow or high-fat (45 energy% of fat derived from palm oil; Research Diet Services BV, Wijk bij Duurstede, The Netherlands)). All animal experiments were performed in accordance with the regulations of Dutch law on animal welfare and the institutional ethics committee for animal procedures from the Leiden University Medical Center, Leiden, The Netherlands approved the protocol.

Surgical procedure

For i.c.v. cannula implantation, 15-week-old male mice were anaesthetized with 0.5 mg/kg Medetomidine (Pfizer, Capelle a/d IJssel, The Netherlands), 5 mg/kg Midazolam (Roche, Mijdrecht, The Netherlands) and 0.05 mg/kg Fentanyl (Janssen-Cilag, Tilburg, The Netherlands) and placed in a stereotactic device (TSE systems, Homburg, Germany). A 25 gauge guide cannula was implanted into the left lateral ventricle using the following coordinates from Bregma: 1.0 mm lateral, 0.46 mm posterior and 2.2 mm ventral. The guide cannula was secured to the skull surface with dental cement (GC Europe N.V., Leuven, Belgium) and the anesthesia was antagonized using 2.5 mg/kg Antipamezol (Pfizer, Capelle a/d IJssel, The Netherlands), 0.5 mg/kg Flumazenil (Roche, Mijdrecht, The Netherlands) and 1.2 mg/kg Naloxon (Orpha, Purkersdorf, Austria). After a recovery period of 1 week, cannula placement was verified. Mice that ate >0.3 g in 1 h in response to i.c.v. injection of 5 µg NPY (Bachem, St. Helens, UK) in 1 µl of artificial cerebrospinal fluid (aCSF, Harvard Apparatus, Natick, MA, US) were considered to have the cannula correctly placed and were included in the study (12;13).

Basal and insulin-stimulated glucose metabolism

Postabsorptive (i.e. overnight fasted), body weight-matched male mice were anaesthetized with 6.25 mg/kg Acepromazine (Alfasan, Woerden, The Netherlands), 6.25 mg/kg Midazolam (Roche, Mijdrecht, The Netherlands), and 0.31 mg/kg Fentanyl (Janssen-Cilag, Tilburg, The Netherlands). Tissue-specific glucose uptake was determined, in the basal state and in the hyperinsulinemic-euglycemic state, in separate experiments (Fig. 1). aCSF or the K_{ATP} channel blocker tolbutamide, dissolved in 5% DMSO to a final concentration of 4.8 mM in aCSF, was continuously infused i.c.v. at a rate of 2.5 µl/h using a Harvard infusion pump (7;14). Thirty min after starting the i.c.v. infusion of tolbutamide or vehicle, i.v. infusions were started. In the basal state study, D-[^{14}C]glucose (0.3 µCi/kg/min; Amersham, Little Chalfont, U.K.) was continuously infused for 90 min. In the hyperinsulinemic-euglycemic clamp study, insulin (Actrapid, Novo Nordisk, Denmark) was administered i.v. by primed (4.1 mU), continuous (6.8 mU/h) infusion to attain steady-state insulin levels together with D-[^{14}C]glucose (0.3 µCi/kg/min; Amersham) for 90 min. This infusion rate of insulin was chosen based on previous dose-response studies of hyperinsulinemia, aimed at a five-fold increase in insulin levels which both inhibited EGP and stimulated glucose uptake (15). A variable intravenous infusion of a 12.5% D-glucose solution was used to maintain euglycemia as determined at 10-min intervals via tail bleeding (< 3 µl, Accu-chek, Sensor Comfort; Roche Diagnostics, Mannheim, Germany). In a separate experiment, aCSF or the K_{ATP} channel activator diazoxide (dissolved in 5% DMSO, to a final concentration of 2 µg/µl in aCSF) was continuously infused i.c.v. in high-fat fed mice during hyperinsulinemic-euglycemic clamp. To assess basal and insulin-mediated glucose uptake in individual tissues, 2-deoxy-D-[^{3}H]glucose (2-[^{3}H]DG; Amersham) was administered as a bolus (1 µCi) 30 min before the end of both experiments. In the last 20 min of both experiments, blood samples were taken with intervals of 10 min. Subsequently, the mice were sacrificed, perfused with PBS and organs were quickly harvested and snap-frozen in liquid nitrogen.

Plasma analysis

Blood samples were taken from the tail tip into chilled paraoxon-coated capillaries to prevent *ex vivo* lipolysis. The tubes were placed on ice and centrifuged at 4°C. Plasma levels of glucose and free fatty acids (FFA) were determined using commercially available kits and standards according to the instructions of the manufacturer (Instruchemie, Delfzijl, The Netherlands). Plasma insulin levels were measured using a mouse-specific insulin ELISA kit (Crystal Chem Inc., Downers Grove, U.S.). Total plasma ^{14}C-glucose and ^{3}H-glucose were determined in supernatant of 7.5 µl plasma, after protein precipitation using 20% trichloroacetic acid and evaporation to eliminate tritiated water.

Tissue analysis

For determination of tissue 2-[^{3}H]DG uptake, homogenates of brain, heart, skeletal muscle (upper hindlimb) and WAT (epigonadal, visceral and subcutaneous) were boiled, and the supernatants were subjected to an ion-exchange column to separate 2-[^{3}H]DG-6-phosphate (which is trapped within the organ and not phosphorylated) from 2-[^{3}H]DG as described previously (16-18).

Calculations

Turnover rates of glucose (µmol/min/kg) were calculated for the basal state and for the hyperinsulinemic-euglycemic state as the rate of tracer infusion (dpm/min) divided by plasma specific activities of ^{14}C-glucose (dpm/µmol). The ratio was corrected for body weight. EGP was calculated as the difference between the tracer-derived rate of glucose appearance and the glucose infusion rate.

Tissue-specific glucose uptake in brain, muscle and WAT was calculated from tissue 2-[^{3}H]DG content, corrected for plasma specific activity and expressed as micromoles per gram of tissue.

Western blot analysis

Whole hypothalami and skeletal muscles (upper hindlimb) of mice receiving i.c.v. aCSF in basal state and hyperinsulinemic-euglycemic state (n=5) were homogenized by Ultra-Turrax (22.000 rpm; 2x5 sec) in a 6:1 (v/w) ratio of ice-cold buffer containing: 50 mM HEPES (pH 7.6), 50 mM NaF, 50 mM KCl, 5 mM *TSPP (sodium pyrophosphate)*, 1 mM EDTA, 1 mM EGTA, 5 mM β-GP, 1 mM Na3VO4, 1 mM DTT, 1% NP40 and protease inhibitors cocktail (Complete, Roche, Mijdrecht, The Netherlands). Homogenates were centrifuged (13, 200 rpm; 15 min, 4°C) and the protein content of the supernatant was determined using a bicinchoninic acid (BCA) protein assay kit (BCA Protein Assay Kit, Thermo Scientific Pierce Protein Research Products, Rockford, US). Proteins (20-50 µg) were separated by 7-10% SDS-PAGE followed by transfer to a PVDF transfer membrane. Membranes were blocked for 1 h at room temperature in Tris-buffered saline with Tween-20 buffer and 5% non-fat dry milk followed by an overnight incubation with phospho-specific or total antibodies (all from Cell Signaling Technology, Beverly, US). Blots were then incubated with HRP-conjugated secondary antibodies for 1 h at room temperature. Bands were visualized by enhanced chemiluminescence and quantified using Image J (NIH, US).

Statistical analysis

Differences between groups were determined by Mann-Whitney nonparametric tests for two independent samples. The criterion for significance was set at $P < 0.05$. All values shown represent means ± SEM.

RESULTS

I.c.v. tolbutamide administration in post-absorptive, chow fed mice

Plasma parameters and body weight

The design of the infusion studies is shown in Figure 1. In the basal and in the hyperinsulinemic state, body weight, plasma glucose, FFA and insulin levels did not differ between tolbutamide- and vehicle-treated chow fed mice (Table 1). As expected, in the hyperinsulinemic-euglycemic state, insulin levels were five-fold higher and FFA levels were ~50% lower than the values in the basal state, both in the tolbutamide- and vehicle-treated groups. In agreement with the rise in plasma insulin levels, hypothalamic insulin signaling was activated in the hyperinsulinemic-euglycemic state as phosphorylation of PKB on Thr308 (1.2 ± 0.1 *vs*. 1.0 ± 0.1, $P = 0.08$) and its downstream target PRAS40 on Thr246 (1.5 ± 0.1 *vs*. 1.0 ± 0.1, $P < 0.05$) were increased compared to basal state (Fig. 2).

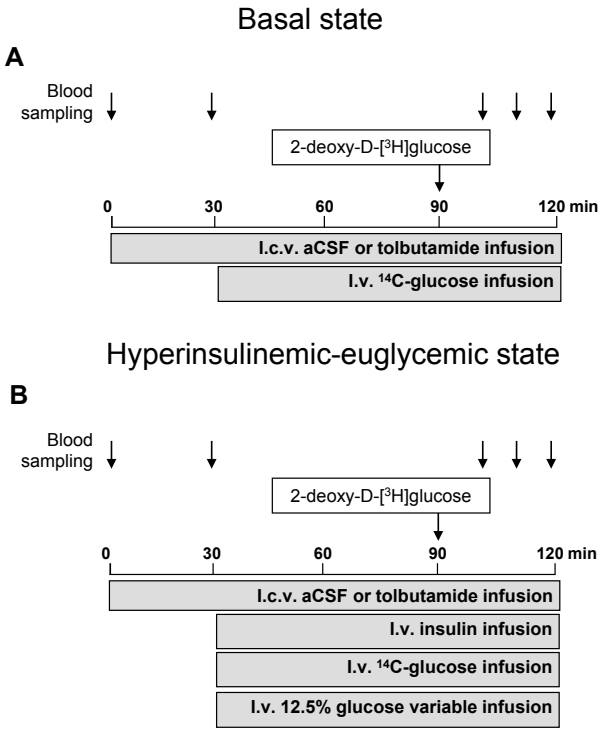

Fig. 1. Schematic representation of the experimental procedures. (A) Basal state. At t=0 min, a continuous i.c.v. infusion of vehicle or tolbutamide was started and maintained throughout the entire experiment. At t=30 min, a primed, continuous i.v. infusion of ^{14}C-glucose was initiated and maintained for the remainder of the experiment. At t=90 min, an i.v. bolus of 2-[^{3}H]DG was administered. At t=0, 100, 110 and 120 min, blood samples were obtained and at t=120 min, the animals were sacrificed and organs harvested. (B) Hyperinsulinemic-euglycemic state. At t=0 min, a continuous i.c.v. infusion of vehicle or tolbutamide was started and maintained throughout the entire experiment. At t=30 min, a hyperinsulinemic-euglycemic clamp was started by primed, continuous infusion of insulin together with ^{14}C-glucose. A variable infusion of 12.5% glucose was used to maintain euglycemia. At t=90 min, an i.v. bolus of 2-[^{3}H]DG was administered. At t=0, 100, 110 and 120 min, blood samples were obtained and at t=120 min, the animals were sacrificed and organs harvested.

Table 1. Plasma parameters of chow fed mice, in basal or hyperinsulinemic-euglycemic state, as measured at the end of the experiments. Throughout the experiments, mice received i.c.v. infusion of vehicle or tolbutamide. Values are means ± SEM for at least 8 mice per group. FFA, free fatty acids. * $P < 0.01$ basal *vs*. hyperinsulinemic state.

	Basal state		**Hyperinsulinemic state**	
	vehicle	**tolbutamide**	**vehicle**	**tolbutamide**
Body weight (g)	23.5 ± 0.4	23.6 ± 0.4	22.8 ± 0.2	22.8 ± 0.5
Glucose (mmol/l)	5.2 ± 0.2	5.8 ± 0.4	6.2 ± 0.5	6.4 ± 0.5
FFA (mmol/l)	0.6± 0.1	0.6 ± 0.1	0.3 ± 0.1 *	0.3 ± 0.1 *
Insulin (ng/ml)	0.9 ± 0.1	1.0 ± 0.1	5.5 ± 0.4 *	4.9 ± 0.2 *
Hematocrit (%)	44.1 ± 0.7	44.3 ± 1.0	42.2 ± 0.6	42.5 ± 1.1

Glucose infusion rate

In the hyperinsulinemic-euglycemic clamp study, the rate of glucose infusion (GIR) necessary to maintain euglycemia was significantly lower in tolbutamide-treated animals compared to vehicle-treated animals (average GIR 87 ± 6 *vs*. 104 ± 13 µmol/min/kg for the last 20 min of the experiment, $P < 0.05$, Fig. 3A), in the presence of similar glucose levels (average plasma glucose 5.4 ± 0.2 *vs*. 5.6 ± 0.1 mmol/l for the last 20 min of the experiment, ns, Fig. 3B), indicating that i.c.v. tolbutamide decreased insulin sensitivity. The glucose specific activities measured at 10 min intervals in all experiments indicated the presence of steady-state conditions in all groups (Table 2).

Endogenous glucose production and glucose disposal

In the basal state, endogenous glucose production (EGP), which equals glucose disposal, was not different between i.c.v. tolbutamide- and i.c.v vehicle-treated animals (36 ± 4 *vs*. 30 ± 2 µmol/min/kg, respectively, ns, Fig. 4A). In the hyperinsulinemic-euglycemic state, EGP was significantly decreased compared to the basal state (1 ± 1 *vs*. 30 ± 2 µmol/min/kg, respectively, $P < 0.01$). I.c.v. tolbutamide in the hyperinsulinemic state diminished the inhibitory effects of insulin on EGP (12 ± 4 *vs*. 1 ± 1 µmol/min/kg, $P < 0.05$).

Table 2. Specific activity of glucose (dpm/mmol) in the postabsorptive state or in the hyperinsulinemic euglycemic state of chow-fed mice. Throughout the experiment, mice received i.c.v. infusion of aCSF or tolbutamide. Values are means ± SEM for at least 8 mice per group.

	Postabsorptive state		
	100 min	**110 min**	**120 min**
vehicle	$11.9 \pm 0.4 \times 10^3$	$11.4 \pm 0.9 \times 10^3$	$11.8 \pm 0.5 \times 10^3$
tolbutamide	$11.0 \pm 1.1 \times 10^3$	$11.3 \pm 0.9 \times 10^3$	$9.4 \pm 1.1 \times 10^3$
	Hyperinsulinemic state		
	100 min	**110 min**	**120 min**
vehicle	$4.1 \pm 0.5 \times 10^3$	$4.0 \pm 0.7 \times 10^3$	$4.3 \pm 1.6 \times 10^3$
tolbutamide	$4.1 \pm 0.3 \times 10^3$	$3.8 \pm 0.2 \times 10^3$	$4.2 \pm 0.3 \times 10^3$

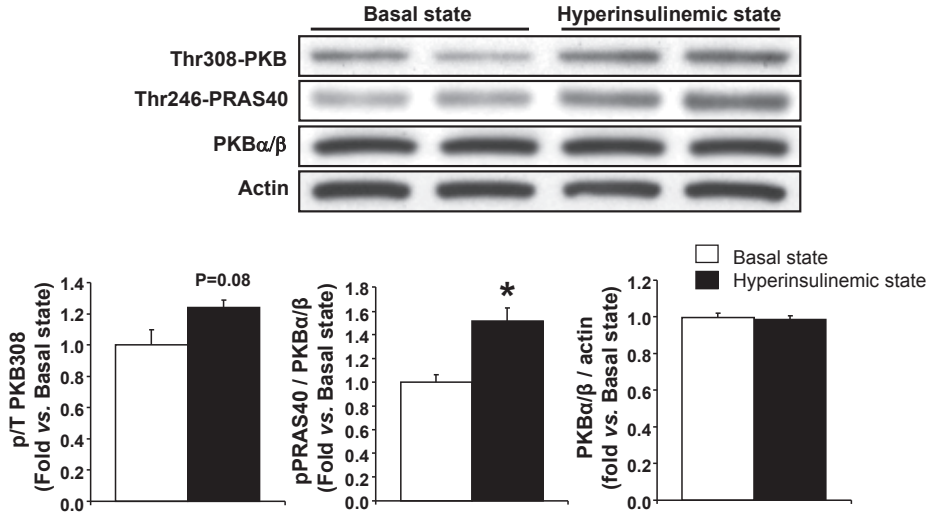

Fig. 2. Phosphorylation state of PKB and PRAS40 in basal state (white bars) or hyperinsulinemic-euglycemic state (black bars) in hypothalamus of chow fed mice. The corresponding quantification of the western blot data was normalized for total protein or actin and expressed as fold change compared to basal state. Values represent means ± SEM for 5 mice per group. * $P < 0.05$ *vs.* vehicle.

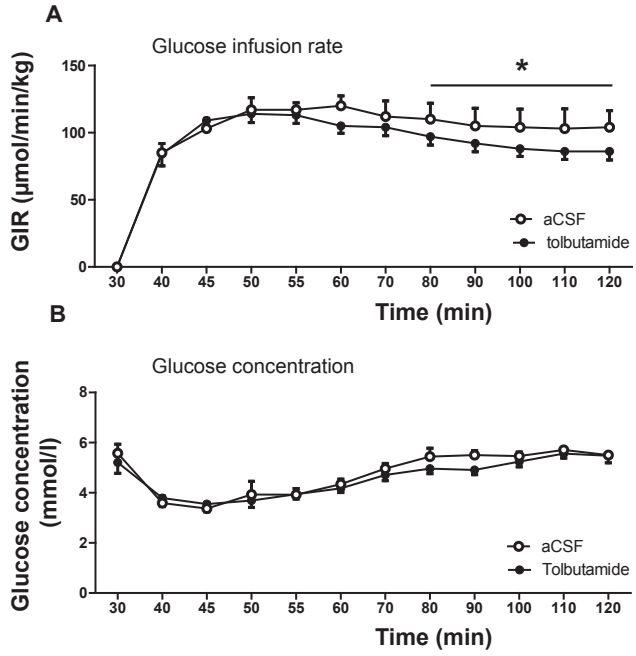

Fig. 3. Glucose infusion rates (GIR, A) and glucose concentrations (B) during hyperinsulinemic-euglycemic clamp in chow fed mice. Throughout the experiment, mice received i.c.v. infusion of vehicle (open circles) or tolbutamide (closed circles). Values represent means ± SEM for at least 8 mice per group. *$P < 0.05$, vehicle *vs.* tolbutamide.

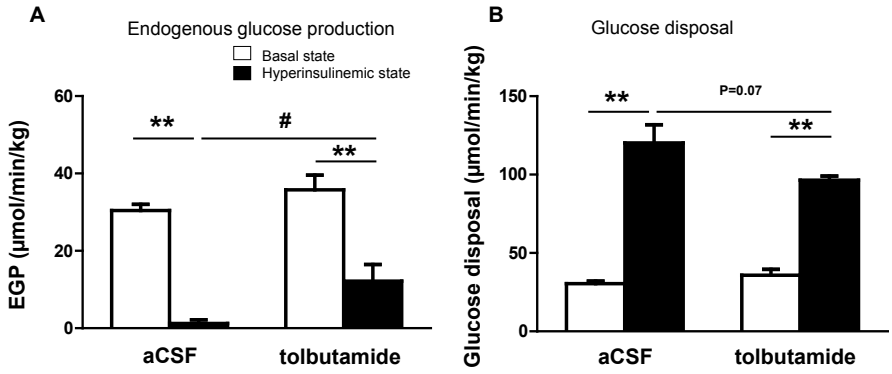

Fig. 4. Rates of endogenous glucose production (EGP, A) and glucose disposal (B) in basal state (white bars) or hyperinsulinemic-euglycemic state (black bars) in chow fed mice. Throughout the experiment, mice received i.c.v. infusion of vehicle or tolbutamide. Values represent means ± SEM for at least 8 mice per group. $^{**}P < 0.01$ basal vs. hyperinsulinemic state, $^{\#}P < 0.05$, hyperinsulinemic state: vehicle *vs*. tolbutamide.

Glucose disposal was increased by ~300% in the hyperinsulinemic-euglycemic state compared to the basal state (120 ± 12 *vs*. 30 ± 2 µmol/min/kg, respectively, $P < 0.01$, Fig. 4B), whereas i.c.v. tolbutamide in the hyperinsulinemic state tended to reduce glucose disposal (97 ± 3 *vs*. 120 ± 12 µmol/min/kg, $P = 0.07$).

Tissue-specific glucose uptake

In the basal and hyperinsulinemic-euglycemic states, 2-[^{3}H]DG uptake was measured in brain, muscle (cardiac and skeletal) and WAT (epigonadal, subcutaneous and visceral fat) (Fig. 5). In brain, 2-[^{3}H]DG uptake did not differ between the basal and the hyperinsulinemic states (12 ± 2 *vs*. 15 ± 4 µmol/g tissue, respectively, ns) and was not affected by i.c.v. tolbutamide (11 ± 1 *vs*. 14 ± 1 µmol/g tissue for basal and hyperinsulinemic state, respectively, ns). In heart, insulin increased 2-[^{3}H]DG uptake six-fold in the hyperinsulinemic state compared to the rate of uptake measured in the basal state (12 ± 1 *vs*. 2 ± 1 µmol/g tissue, respectively, $P < 0.05$), but this increase was not affected by i.c.v. tolbutamide. In muscle, insulin increased 2-[^{3}H]DG uptake considerably in the hyperinsulinemic state compared to the basal state (11 ± 3 *vs*. 1 ± 1 µmol/g tissue, respectively, $P < 0.05$). Remarkably, i.c.v. tolbutamide inhibited the insulin-mediated increase in 2-[^{3}H]DG uptake by muscle by ~59% (5 ± 1 *vs*. 11± 3 µmol/g tissue, $P < 0.05$). Phosphorylation of PKB on Ser473 (14 ± 1 *vs*. 14 ± 1, ns) and Thr308 (8 ± 1 *vs*. 8 ± 1, ns) and its downstream target PRAS40 on Thr246 (14 ± 1 *vs*. 12 ± 1, ns) were not different between i.c.v. vehicle and i.c.v. tolbutamide infused mice in hyperinsulinemic conditions (Fig. 6). In all fat pads, insulin stimulated 2-[^{3}H]DG uptake in the hyperinsulinemic state compared to the basal state, but this increase was not affected by i.c.v. tolbutamide.

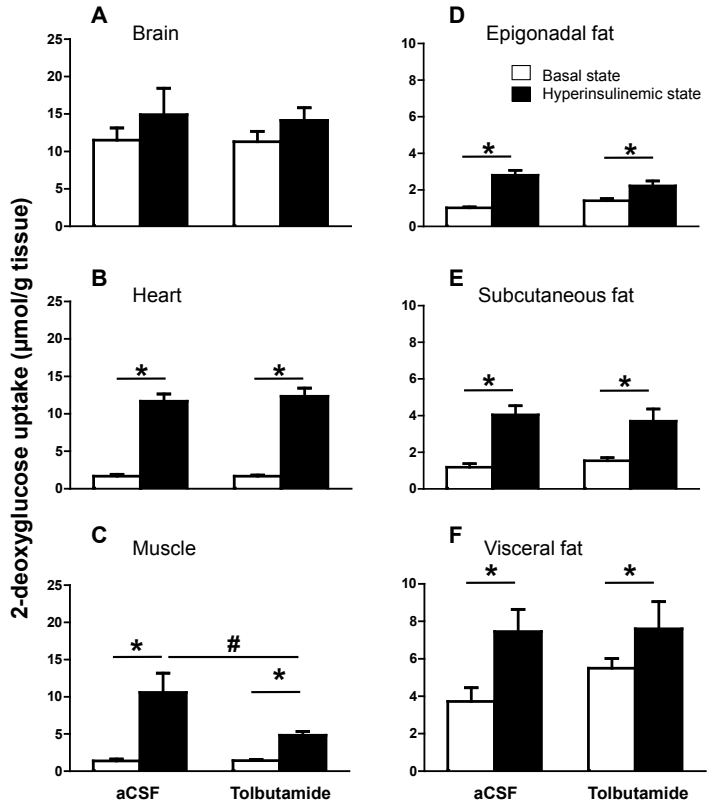

Fig. 5. Tissue-specific glucose uptake in basal state (white bars) or hyperinsulinemic-euglycemic state (black bars) in chow fed mice. Throughout the experiment, mice received i.c.v. infusion of vehicle or tolbutamide. Values represent means ± SEM for at least 7 mice per group. *$P < 0.05$ basal *vs.* hyperinsulinemic state, #$P < 0.05$, hyperinsulinemic state: vehicle *vs.* tolbutamide.

Table 3. Plasma parameters of diet-induced obese mice, in basal or hyperinsulinemic-euglycemic state, as measured at the end of the experiments. Throughout the experiments, mice received i.c.v. infusion of vehicle or tolbutamide. Values are means ± SEM for at least 6 mice per group. FFA, free fatty acids. * $P < 0.01$ basal *vs.* hyperinsulinemic state.

	Basal state	**Hyperinsulinemic state**	
	vehicle	**vehicle**	**tolbutamide**
Body weight (g)	36.4 ± 0.8	37.6 ± 1.5	37.4 ± 0.7
Glucose (mmol/l)	5.1 ± 0.4	5.8 ± 0.4	6.2 ± 0.3
FFA (mmol/l)	0.7 ± 0.1	0.3 ± 0.1 *	0.3 ± 0.1 *
Insulin (ng/ml)	1.4 ± 0.4	7.5 ± 0.5 *	7.9 ± 0.6 *
Hematocrit (%)	44.3 ± 0.6	42.2 ± 1.0	42.4 ± 0.8

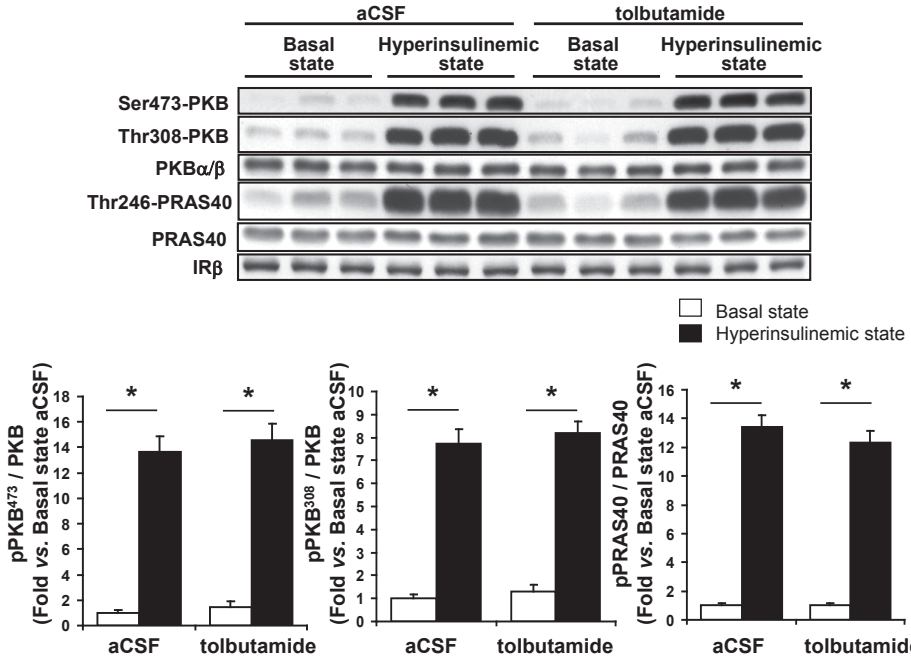

Fig. 6. Phosphorylation state of PKB and PRAS40 in basal state (white bars) or hyperinsulinemic-euglycemic state (black bars) in muscle of chow fed mice receiving i.c.v. infusion of vehicle or tolbutamide. The corresponding quantification of the western blot data was normalized for total protein and expressed as fold change compared to basal state. Values represent means ± SEM for 5 mice per group. * $P < 0.05$ *vs.* vehicle.

I.c.v. tolbutamide administration in postabsorptive, diet-induced obese mice

Plasma parameters and body weight

Since all parameters in the basal state were not different between i.c.v tolbutamide- and i.c.v. vehicle-treated animals in chow fed conditions, we assessed the effects of i.c.v. tolbutamide in high-fat treated mice only in hyperinsulinemic-euglycemic clamp conditions. Body weight of the diet-induced obese mice was markedly higher compared to chow fed mice (37 ± 1 *vs.* 23 ± 1 g, respectively, $P < 0.01$, Table 3). Plasma glucose and hematocrit levels were similar in basal and hyperinsulinemic conditions. In the hyperinsulinemic-euglycemic state, insulin levels were five-fold higher compared to the basal state, resulting in a decrease of ~50% in FFA levels. There were no differences observed in body weight, plasma glucose, FFA, insulin and hematocrit levels between i.c.v. tolbutamide- and i.c.v. vehicle-treated animals in the hyperinsulinemic-euglycemic state.

Endogenous glucose production and glucose disposal

The GIR necessary to maintain euglycemia, was not different between tolbutamide- and vehicle-treated animals (Fig. 7). Plasma glucose specific activities obtained during the last 20 min of the experiments indicated the presence of steady-state conditions in all groups (Table 4).

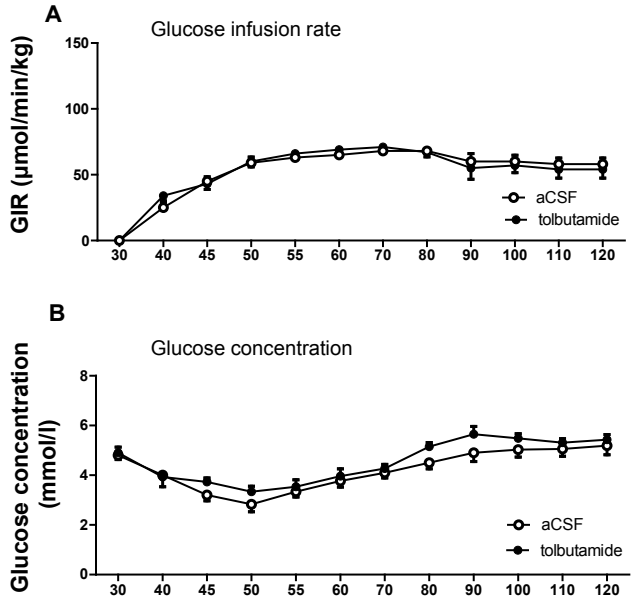

Fig. 7. Glucose infusion rates (GIR, A) and glucose concentrations during a hyperinsulinemic-euglycemic clamp (B) in diet-induced obese mice. Throughout the experiment, mice received i.c.v. infusion of aCSF (open circles) or tolbutamide (closed circles). Values represent mean ± SEM for at least 7 mice per group.

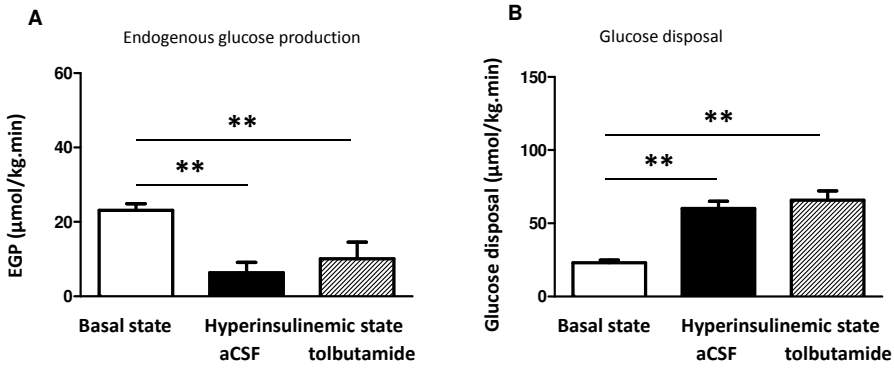

Fig. 8. Rates of endogenous glucose production (EGP, A) and glucose disposal (B) in basal state (white bars) or hyperinsulinemic-euglycemic state (black and hatched bars) in diet-induced obese mice. Throughout the experiment, mice received an i.c.v. infusion of vehicle (white and black bars) or tolbutamide (hatched bars). Values represent means ± SEM for at least 7 mice per group. $^{**}P < 0.01$ basal *vs.* hyperinsulinemic state.

In the hyperinsulinemic-euglycemic state, insulin decreased EGP compared to the basal state by ~74% (6 ± 3 *vs.* 23 ± 2 µmol/min/kg, respectively, $P < 0.01$, Fig. 8A), but surprisingly i.c.v. tolbutamide did not attenuate this effect of insulin in these diet-induced mice (i.c.v. tolbutamide- *vs.* i.c.v. vehicle-treated animals: 10.0 ± 4 *vs.* 6.3 ± 3 µmol/min/kg, ns).

Table 4. Specific activity of glucose (dpm/mmol) in the postabsorptive state or in the hyperinsulinemic euglycemic state of high fat diet-induced obese mice. Throughout the experiment, i.c.v. tolbutamide or aCSF was administered. Values are means ± SEM for at least 8 mice per group.

	Postabsorptive state		
	100 min	**110 min**	**120 min**
vehicle	$11.2 \pm 0.9 \times 10^3$	$11.1 \pm 0.7 \times 10^3$	$14.0 \pm 1.0 \times 10^3$
	Hyperinsulinemic state		
	100 min	**110 min**	**120 min**
vehicle	$4.0 \pm 0.4 \times 10^3$	$4.3 \pm 0.5 \times 10^3$	$4.3 \pm 0.3 \times 10^3$
tolbutamide	$4.6 \pm 0.4 \times 10^3$	$4.2 \pm 0.3 \times 10^3$	$4.3 \pm 0.2 \times 10^3$

In the hyperinsulinemic-euglycemic state, insulin increased glucose disposal only by ~161% compared to the basal state (60 ± 5 *vs*. 23 ± 2 µmol/min/kg, respectively, $P < 0.01$, Fig. 8B). However, this effect of insulin was not affected by i.c.v. tolbutamide (i.c.v. tolbutamide- *vs*. vehicle-treated animals: 62 ± 6 *vs*. 60 ± 5 µmol/min/kg, ns).

Comparison of the data from this experiment with the previously mentioned chow fed experiments indicated that the obese mice were considerably insulin resistant. Muscle glucose uptake under hyperinsulinemic-euglycemic conditions in high-fat fed mice was significantly lower compared to chow fed mice (7.9 ± 1.1 *vs*. 10.6 ± 2.6 µmol/min/kg, $P < 0.05$). In addition, glucose disposal rate was lower (60.2 ± 4.9 *vs*. 120.1 ± 11.7 µmol/min/kg, $P < 0.05$) and EGP was higher (6.4 ± 2.8 *vs*. 1.2 ± 1.0 µmol/min/kg, $P < 0.05$), indicating both hepatic and peripheral insulin resistance in the diet-induced obese mice.

Tissue-specific glucose uptake

In diet-induced obese mice, we measured tissue-specific 2-[^{3}H]DG uptake in brain, muscle (cardiac and skeletal) and WAT (epigonadal, subcutaneous and visceral fat) in the basal state and in the hyperinsulinemic-euglycemic state (Fig. 9). In muscle, insulin stimulated 2-[^{3}H]DG uptake compared to the basal state (8 ± 1 *vs*. 2 ± 1 µmol/g tissue, respectively, $P < 0.05$). In contrast to chow fed mice, in diet-induced obese mice there was no effect of i.c.v. tolbutamide on insulin-mediated muscle glucose uptake. In accordance with the observation in chow fed mice, insulin increased 2-[^{3}H]DG uptake in the hyperinsulinemic state compared to the basal state in heart and WAT, but not in brain, whereas i.c.v. tolbutamide did not affect 2-[^{3}H]DG uptake in any of these organs.

I.c.v. diazoxide administration in postabsorptive, diet-induced obese mice

In high-fat fed mice we assessed the effects of i.c.v. diazoxide, a K_{ATP} channel activator, on insulin-stimulated muscle glucose uptake (Table 5). There were no differences observed in body weight and plasma glucose between i.c.v. diazoxide and vehicle treated animals. The GIR necessary to maintain euglycemia, glucose disposal and 2-[^{3}H]DG uptake by muscle was not different between i.c.v. diazoxide and vehicle treated animals.

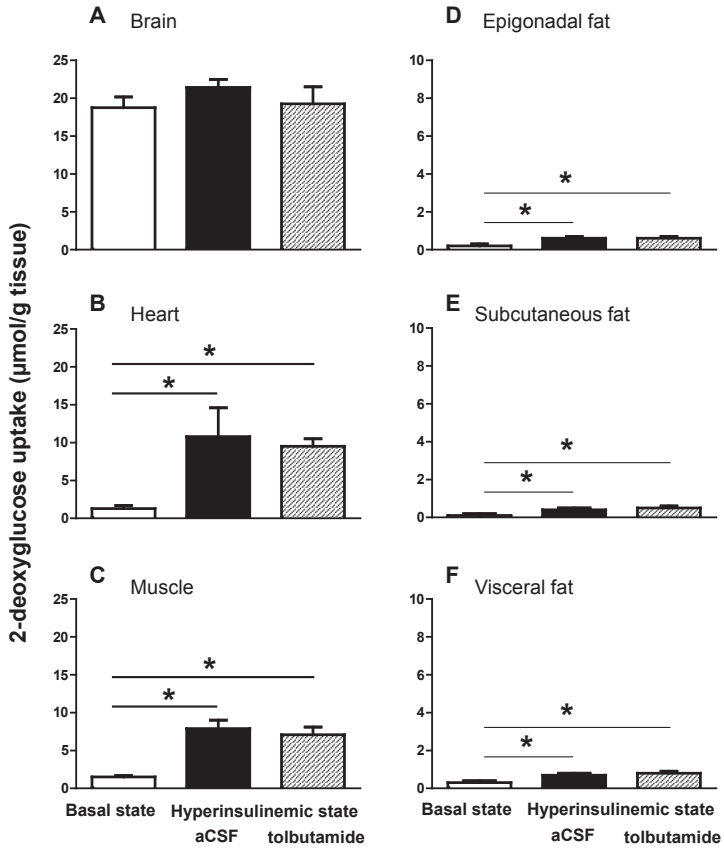

Fig. 9. Tissue-specific glucose uptake in basal state (white bars) or hyperinsulinemic-euglycemic state (black and hatched bars) in diet-induced obese mice. Throughout the experiment, mice received i.c.v. infusion of vehicle (white and black bars) or tolbutamide (hatched bars). Values represent means ± SEM for at least 7 mice per group. *$P < 0.05$ basal *vs.* hyperinsulinemic state.

Table 5. Plasma parameters of high-fat fed mice, in hyperinsulinemic-euglycemic state. Throughout the experiments, mice received i.c.v. infusion of vehicle or diazoxide. Values are means ± SEM for at least 5 mice per group.

	Hyperinsulinemic state	
	vehicle	**diazoxide**
Body weight (g)	31.3 ± 1.7	30.8 ± 0.3
Glucose (mmol/l)	5.6 ± 0.2	5.2 ± 0.4
GIR (µmol/min/kg)	52.4 ± 4.8	54.3 ± 4.6
Glucose disposal (µmol/min/kg)	52.7 ± 4.3	52.1 ± 5.0
Muscle glucose uptake (µmol/g tissue)	7.7 ± 0.7	7.8 ± 0.5

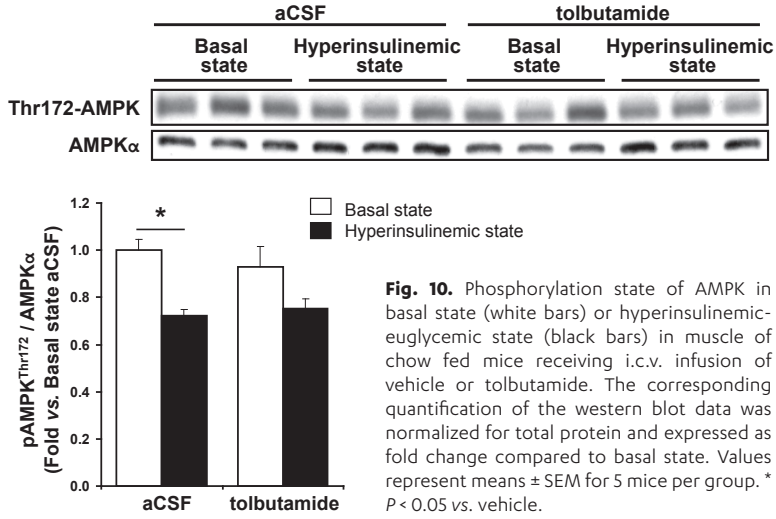

Fig. 10. Phosphorylation state of AMPK in basal state (white bars) or hyperinsulinemic-euglycemic state (black bars) in muscle of chow fed mice receiving i.c.v. infusion of vehicle or tolbutamide. The corresponding quantification of the western blot data was normalized for total protein and expressed as fold change compared to basal state. Values represent means ± SEM for 5 mice per group. * $P < 0.05$ *vs.* vehicle.

DISCUSSION

This study addressed the effect of central antagonism of insulin signaling on tissue-specific glucose uptake in normal weight and diet-induced obese mice. Inhibition of the central action of insulin by i.c.v. tolbutamide, a K_{ATP} channel blocker, decreased the inhibitory effects of insulin on EGP as well as the insulin-stimulated muscle glucose uptake in chow fed mice. In contrast, in diet-induced obese mice, the effects of insulin on EGP and muscle glucose uptake were not affected by i.c.v. tolbutamide. Collectively, these data indicate that the central effects of insulin are not only required for inhibition of EGP, but also for muscle glucose uptake. In addition, these data indicate that these central effects of insulin on EGP and muscle glucose uptake are absent after 12 weeks of high-fat feeding.

We assessed insulin-mediated effects on EGP and glucose disposal by hyperinsulinemic-euglycemic clamp studies designed to increase plasma insulin concentrations by approximately five-fold above basal levels. This increase resulted in complete inhibition of EGP and a four-fold stimulation of glucose disposal. In complete accordance with the results of Obici *et al*. (7), i.c.v. tolbutamide blunted the effect of hyperinsulinemia on EGP by ~20%. Therefore, this observation confirms that insulin inhibits EGP in part via its action in the CNS. In addition, our results indicate that the central effects of insulin contribute to the stimulatory effects of insulin on muscle glucose uptake, since this effect of insulin was in part inhibited (~59%) by i.c.v. tolbutamide. This inhibition of muscle glucose uptake coincided with a trend in decreased whole body glucose disposal (~20%, $P = 0.07$), which did not reach statistical significance probably due to the limited size of the mouse groups.

The present study indicates that i.c.v. tolbutamide decreased insulin-stimulated muscle glucose uptake in chow fed mice, not by decreasing insulin signaling in skeletal muscle as phosphorylation of PKB and PRAS40 were unaffected by i.c.v. tolbutamide, but, through other, indirect, effects of insulin exerted via the CNS. A role of central insulin signaling in

muscle glucose uptake has been suggested in a previous study on cerebral control of muscle glucose uptake (19). In that study, i.c.v. insulin increased glucose storage in muscle as glycogen. Together with the results obtained in our study, a concept emerges of an insulin-dependent central pathway targeted at skeletal muscle. I.c.v. NPY or AgRP did not stimulate muscle glucose uptake (20). Chronic (7-day) i.c.v. infusion of a-MSH, a POMC derivative, enhanced insulin-stimulated peripheral glucose uptake, although this effect could not be reproduced in an acute setting (21;22). However, i.c.v. infusion of melanotan II, a MC3/4 agonist, enhanced insulin-stimulated muscle glucose uptake (23;24). Therefore, we hypothesize that POMC/CART neurons are potential mediators of the central effect of insulin on muscle glucose uptake.

Previous studies focusing on the role of central K_{ATP} channels in glucose metabolism could not show an effect on glucose disposal (7;11). There are some methodological differences between the studies, including insulin levels and duration of fasting. In previous experiments, we carefully characterized insulin dose-response characteristics on EGP *vs*. glucose disposal in C57Bl/6J mice (14). The data obtained in this dose-finding study indicate that increased insulin levels up to three times the basal levels inhibit EGP, but do not stimulate glucose disposal. Therefore, in the current study we aimed at five-fold increased insulin levels during the clamp as compared to the basal levels, compared to two- to three-fold levels in previous studies (6;11). Using these insulin levels, we were not only capable in reproducing the central effects of insulin on EGP as reported by Obici *et al.*, but in addition to document central effects of insulin on muscle glucose uptake. Therefore, we speculate that the discrepancy in the effects of central K_{ATP} channel modulation on insulin-mediated glucose uptake during hyperinsulinemia between our study and previous studies is explained by the higher insulin levels in our study. Furthermore, Obici *et al*. (7) studied rats fasted for 6 hours and did not find an inhibition of glucose disposal rate by i.c.v. administration of tolbutamide, in contrast to our observations in overnight fasted mice. In a previous study, we documented that 16 h of (overnight) fasting increases muscle insulin sensitivity compared to a shorter duration of fasting (25). Therefore, differences between the duration of fasting may be involved to explain the differential effects of i.c.v. tolbutamide on insulin-stimulated glucose uptake between both studies. Nonetheless, this does not invalidate our conclusions, since the duration of fast was identical in all experiments of our study.

Glucose utilization in skeletal muscle can be stimulated by sympathetic nervous system (SNS) activation and i.c.v. insulin in rats increases SNS activity to the hindlimb (26). Therefore, the observed effect on insulin-mediated glucose uptake in muscle following central K_{ATP} channel inhibition could be the result of reduced insulin-induced activation of the SNS towards muscle. Since the stimulation of muscle glucose uptake by α-adrenergic stimulation involves 5'-AMP-activated protein kinase (AMPK), we measured AMPKα phosphorylation in muscle (27). However, i.c.v. infusion of insulin or K_{ATP} channel inhibition under hyperinsulinemic conditions did not affect activity of AMPK in muscle (Fig. 10). Apparently, the stimulation of muscle glucose uptake by central insulin effects is independent of AMPK activation in muscle. At present, the involvement of autonomic pathways in mediating the central effects of insulin on muscle glucose uptake remains unclear.

Insulin stimulated glucose uptake in heart and WAT. Interestingly, this effect of insulin was greater in visceral fat compared to the other fat compartments, in accordance with previous observations (28-30). The insulin-stimulated glucose uptake by heart and WAT was independent

of central K_{ATP} channel activation, since i.c.v. tolbutamide did not affect tissue-specific glucose uptake in these tissues.

We also assessed the effects of high-fat diet on the central effects of insulin on EGP and tissue-specific glucose uptake. The study was designed for the mice to develop obesity in combination with partial, rather than complete, insulin resistance, and, as a result, effects of central insulin antagonism in these diet-induced obese mice could still be obtained. Indeed, the high-fat diet caused partial insulin resistance, since insulin was still able, although to a lesser extent, to inhibit EGP and stimulate glucose disposal. The high-fat diet abolished the inhibitory effect of i.c.v. tolbutamide on insulin-mediated inhibition of EGP. Furthermore, the inhibitory effect of i.c.v administration of tolbutamide on insulin-stimulated glucose uptake by skeletal muscle was abolished. Our *in vivo* observations in diet-induced obese mice extend the *in vitro* observations by Spanswick *et al.*, showing that physiological levels of insulin activate K_{ATP} channels in glucose responsive neurons of lean, but not of obese rats, suggesting that K_{ATP} channels are already inhibited in the insulin resistant state (10;31-33). Moreover, stimulation of K_{ATP} channels by i.c.v. diazoxide did not improve muscle glucose uptake under hyperinsulinemic-euglycemic clamp conditions in diet-induced obese insulin resistant mice. The absence of effects of i.c.v. tolbutamide in diet-induced obese mice might also involve reduced insulin transport across the blood brain barrier (34). Although the precise mechanism remains to be elucidated, the present study indicates that high-fat diet decreases the central effects of insulin on both EGP and muscle glucose uptake, which may contribute to the pathophysiology of diet-induced insulin resistance. High-fat feeding strongly reduced insulin-stimulated glucose disposal, indicating peripheral insulin resistance. Interestingly, in quantitative terms, insulin-stimulated muscle glucose uptake in chow fed conditions during i.c.v. tolbutamide infusion, was not different from muscle glucose uptake during high-fat conditions (5.2 ± 0.6 *vs.* 7.1 ± 1.0 µmol/g tissue, ns). This remarkable observation indicates that muscle-specific insulin resistance was present for the centrally mediated effects of insulin, rather than for the direct effects of insulin on muscle, at least within the constraints of our high-fat diet mouse model.

Recently, methodological issues have been raised concerning the application of the hyperinsulinemic-euglycemic clamp method in mice (35). To support the validity of our experimental procedures, we documented that we reached steady-state conditions with respect to GIR, plasma glucose concentrations and isotopes, the latter enabling reliable calculations using steady-state comparisons. Another issue that has been raised is that the mice may be subject to serious hemodilution during the clamps. Our data indicate that hemodilation hardly occurred at the end of the clamps in our mice as hematocrit levels remained similar. Furthermore, our clamp procedure was performed in anesthetized mice. However, since all groups received identical sedation, the differences between groups cannot be related to sedation.

Recently, we also documented central effects of insulin on FA uptake (12). Those studies show that i.c.v. tolbutamide administration in hyperinsulinemic-euglycemic clamp conditions, identical to the current conditions, decreases insulin-stimulated retention of FA specifically in WAT. Therefore, the notion emerges that regulation of FA and glucose uptake by modulation of central insulin signaling is tissue-specific. In addition, both

studies indicate that these effects are mediated, at least in part, via K_{ATP} channel activation in the CNS and are absent after high-fat feeding.

We conclude that insulin signaling in the brain not only substantially contributes to the inhibitory effect of insulin on glucose production, but also to the insulin-stimulated glucose uptake by muscle. In diet-induced obese mice, these central effects of insulin on glucose homeostasis are lost. These observations stress the role of central insulin signaling in normal physiological conditions and central insulin resistance in the pathophysiology of diet-induced insulin resistance.

ACKNOWLEDGEMENTS

This work was supported by grants from TI Pharma (TIP project T2-105, to L.M. Havekes and J.A. Romijn) and ZonMW (Clinical Fellow 90700195, to N.R. Biermasz), the Netherlands Heart Foundation (NHS project 2007B81, to P.C.N. Rensen and J.A. Romijn) and the Dutch Diabetes Research Foundation (DFN project 2007.00.010, to P.C.N. Rensen and J.A. Romijn). P.C.N. Rensen is an Established Investigator of the Netherlands Heart Foundation (NHS2009T038).

REFERENCE LIST

1. DeFronzo, RA, Simonson, D, Ferrannini, E: Hepatic and peripheral insulin resistance: a common feature of type 2 (non-insulin-dependent) and type 1 (insulin-dependent) diabetes mellitus. *Diabetologia* 23:313-319, 1982
2. Hollenbeck, CB, Chen, YD, Reaven, GM: A comparison of the relative effects of obesity and non-insulin-dependent diabetes mellitus on in vivo insulin-stimulated glucose utilization. *Diabetes* 33:622-626, 1984
3. Obici, S, Feng, Z, Karkanias, G, Baskin, DG, Rossetti, L: Decreasing hypothalamic insulin receptors causes hyperphagia and insulin resistance in rats. *Nat Neurosci* 5:566-572, 2002
4. Schwartz, MW, Sipols, AJ, Marks, JL, Sanacora, G, White, JD, Scheurink, A, Kahn, SE, Baskin, DG, Woods, SC, Figlewicz, DP: Inhibition of hypothalamic neuropeptide Y gene expression by insulin. *Endocrinology* 130:3608-3616, 1992
5. Schwartz, MW, Woods, SC, Seeley, RJ, Barsh, GS, Baskin, DG, Leibel, RL: Is the energy homeostasis system inherently biased toward weight gain? *Diabetes* 52:232-238, 2003
6. Fisher, SJ, Bruning, JC, Lannon, S, Kahn, CR: Insulin signaling in the central nervous system is critical for the normal sympathoadrenal response to hypoglycemia. *Diabetes* 54:1447-1451, 2005
7. Obici, S, Zhang, BB, Karkanias, G, Rossetti, L: Hypothalamic insulin signaling is required for inhibition of glucose production. *Nat Med* 8:1376-1382, 2002
8. Okamoto, H, Obici, S, Accili, D, Rossetti, L: Restoration of liver insulin signaling in Insr knockout mice fails to normalize hepatic insulin action. *J Clin Invest* 115:1314-1322, 2005
9. Karschin, C, Ecke, C, Ashcroft, FM, Karschin, A: Overlapping distribution of K(ATP) channel-forming Kir6.2 subunit and the sulfonylurea receptor SUR1 in rodent brain. *FEBS Lett* 401:59-64, 1997
10. Spanswick, D, Smith, MA, Mirshamsi, S, Routh, VH, Ashford, ML: Insulin activates ATP-sensitive K+ channels in hypothalamic neurons of lean, but not obese rats. *Nat Neurosci* 3:757-758, 2000
11. Pocai, A, Lam, TK, Gutierrez-Juarez, R, Obici, S, Schwartz, GJ, Bryan, J, guilar-Bryan, L, Rossetti, L: Hypothalamic K(ATP) channels control hepatic glucose production. *Nature* 434:1026-1031, 2005
12. Coomans, CP, Geerling, JJ, Guigas, B, van den Hoek, AM, Parlevliet, ET, Ouwens, DM, Pijl, H, Voshol, PJ, Rensen, PC, Havekes, LM, Romijn, JA: Circulating insulin stimulates fatty acid retention in white adipose tissue via K_{ATP} channel activation in the central nervous system only in insulin-sensitive mice. *J Lipid Res* 2011
13. van den Hoek, AM, Voshol, PJ, Karnekamp, BN, Buijs, RM, Romijn, JA, Havekes, LM, Pijl,

H: Intracerebroventricular neuropeptide Y infusion precludes inhibition of glucose and VLDL production by insulin. *Diabetes* 53:2529-2534, 2004

14. Plum, L: Enhanced PIP3 signaling in POMC neurons causes K_{ATP} channel activation and leads to diet-sensitive obesity. 2006
15. den Boer, MA, Voshol, PJ, Kuipers, F, Romijn, JA, Havekes, LM: Hepatic glucose production is more sensitive to insulin-mediated inhibition than hepatic VLDL-triglyceride production. *Am J Physiol Endocrinol Metab* 291:E1360-E1364, 2006
16. Parlevliet, ET, Schroder-van der Elst JP, Corssmit, EP, Picha, K, O'Neil, K, Stojanovic-Susulic, V, Ort, T, Havekes, LM, Romijn, JA, Pijl, H: CNTO736, a novel glucagon-like peptide-1 receptor agonist, ameliorates insulin resistance and inhibits very low-density lipoprotein production in high-fat-fed mice. *J Pharmacol Exp Ther* 328:240-248, 2009
17. Rossetti, L, Giaccari, A: Relative contribution of glycogen synthesis and glycolysis to insulin-mediated glucose uptake. A dose-response euglycemic clamp study in normal and diabetic rats. *J Clin Invest* 85:1785-1792, 1990
18. van den Hoek, AM, Teusink, B, Voshol, PJ, Havekes, LM, Romijn, JA, Pijl, H: Leptin deficiency per se dictates body composition and insulin action in ob/ob mice. *J Neuroendocrinol* 20:120-127, 2008
19. Perrin, C, Knauf, C, Burcelin, R: Intracerebroventricular infusion of glucose, insulin, and the adenosine monophosphate-activated kinase activator, 5-aminoimidazole-4-carboxamide-1-beta-D-ribofuranoside, controls muscle glycogen synthesis. *Endocrinology* 145:4025-4033, 2004
20. Shiuchi, T, Haque, MS, Okamoto, S, Inoue, T, Kageyama, H, Lee, S, Toda, C, Suzuki, A, Bachman, ES, Kim, YB, Sakurai, T, Yanagisawa, M, Shioda, S, Imoto, K, Minokoshi, Y: Hypothalamic orexin stimulates feeding-associated glucose utilization in skeletal muscle via sympathetic nervous system. *Cell Metab* 10:466-480, 2009
21. Gutierrez-Juarez, R, Obici, S, Rossetti, L: Melanocortin-independent effects of leptin on hepatic glucose fluxes. *J Biol Chem* 279:49704-49715, 2004
22. Obici, S, Feng, Z, Tan, J, Liu, L, Karkanias, G, Rossetti, L: Central melanocortin receptors regulate insulin action. *J Clin Invest* 108:1079-1085, 2001
23. Heijboer, AC, van den Hoek, AM, Pijl, H, Voshol, PJ, Havekes, LM, Romijn, JA, Corssmit, EP: Intracerebroventricular administration of melanotan II increases insulin sensitivity of glucose disposal in mice. *Diabetologia* 48:1621-1626, 2005
24. Toda, C, Shiuchi, T, Lee, S, Yamato-Esaki, M, Fujino, Y, Suzuki, A, Okamoto, S, Minokoshi, Y: Distinct effects of leptin and a melanocortin receptor agonist injected into medial hypothalamic nuclei on glucose uptake in peripheral tissues. *Diabetes* 58:2757-2765, 2009
25. Heijboer, AC: Sixteen hours of fasting differentially affects hepatic and muscle insulin sensitivity in mice. 2005
26. Rahmouni, K, Morgan, DA, Morgan, GM, Liu, X, Sigmund, CD, Mark, AL, Haynes, WG: Hypothalamic PI3K and MAPK differentially mediate regional sympathetic activation to insulin. *J Clin Invest* 114:652-658, 2004
27. Minokoshi, Y, Kim, YB, Peroni, OD, Fryer, LG, Muller, C, Carling, D, Kahn, BB: Leptin stimulates fatty-acid oxidation by activating AMP-activated protein kinase. *Nature* 415:339-343, 2002
28. Clegg, DJ, Brown, LM, Woods, SC, Benoit, SC: Gonadal hormones determine sensitivity to central leptin and insulin. *Diabetes* 55:978-987, 2006
29. Virtanen, KA, Lonnroth, P, Parkkola, R, Peltoniemi, P, Asola, M, Viljanen, T, Tolvanen, T, Knuuti, J, Ronnemaa, T, Huupponen, R, Nuutila, P: Glucose uptake and perfusion in subcutaneous and visceral adipose tissue during insulin stimulation in nonobese and obese humans. *J Clin Endocrinol Metab* 87:3902-3910, 2002
30. Woods, SC, Gotoh, K, Clegg, DJ: Gender differences in the control of energy homeostasis. *Exp Biol Med (Maywood)* 228:1175-1180, 2003
31. Arase, K, Fisler, JS, Shargill, NS, York, DA, Bray, GA: Intracerebroventricular infusions of 3-OHB and insulin in a rat model of dietary obesity. *Am J Physiol* 255:R974-R981, 1988
32. Ono, H, Pocai, A, Wang, Y, Sakoda, H, Asano, T, Backer, JM, Schwartz, GJ, Rossetti, L: Activation of hypothalamic S6 kinase mediates diet-induced hepatic insulin resistance in rats. *J Clin Invest* 118:2959-2968, 2008
33. Woods, SC, D'Alessio, DA, Tso, P, Rushing, PA, Clegg, DJ, Benoit, SC, Gotoh, K, Liu, M, Seeley, RJ: Consumption of a high-fat diet alters the homeostatic regulation of energy balance. *Physiol Behav* 83:573-578, 2004
34. Kaiyala, KJ, Prigeon, RL, Kahn, SE, Woods, SC, Schwartz, MW: Obesity induced by a high-fat diet is associated with reduced brain insulin transport in dogs. *Diabetes* 49:1525-1533, 2000
35. Wasserman, DH, Ayala, JE, McGuinness, OP: Lost in translation. *Diabetes* 58:1947-1950, 2009